# Hypernuclear physics with FINUDA at DAΦNE

FINUDA Collaboration

M. Agnello [a], G. Beer [b], L. Benussi [c], M. Bertani [c], H.C. Bhang [d], S. Bianco [c], E. Botta [e], M. Bregant [f], T. Bressani [e] L. Busso [g], D. Calvo [h], P. Camerini [f], M. Caponero [i], P. Cerello [h], B. Dalena [j], F. De Mori [e], G. D'Erasmo [j], D. Di Santo [j], R. Donà [k], D. Elia [j], F. L. Fabbri [c], D. Faso [g], A. Feliciello [h], A. Filippi [h], V. Filippini [ℓ,1], R. Fini [j], M. E. Fiore [j], H. Fujioka [m], P. Gianotti [c], N. Grion [n], A. Krasnoperov [o], V. Lucherini [c], V. Lenti [j], V. Manzari [u], S. Marcello [e], T. Maruta [m], N. Mirfakhrai [p], O. Morra [q], T. Nagae [r], A. Olin [s], H. Outa [t], E. Pace [c], M. Pallotta [c], M. Palomba [j], A. Pantaleo [u], A. Panzarasa [ℓ], V. Paticchio [u], S. Piano [f], F. Pompili [c], R. Rui [f], G. Simonetti [j], H. So [d], V. Tereshchenko [o], S. Tomassini [c], A. Toyoda [r], R. Wheadon [h], A. Zenoni [v]

[a] *Dip. di Fisica Politecnico di Torino, via Duca degli Abruzzi Torino, Italy, and INFN Sez. di Torino, via P. Giuria 1 Torino, Italy*

[b] *University of Victoria, Finnerty Rd., Victoria, Canada*

[c] *Laboratori Nazionali di Frascati dell'INFN, via E. Fermi 40 Frascati, Italy*

[d] *Dep. of Physics, Seoul National Univ., 151-742 Seoul, South Korea*

[e] *Dipartimento di Fisica Sperimentale, Università di Torino, via P. Giuria 1 Torino, Italy, and INFN Sez. di Torino, via P. Giuria 1 Torino, Italy*

[f] *Dip. di Fisica Univ. di Trieste, via Valerio 2 Trieste, Italy and INFN, Sez. di Trieste, via Valerio 2 Trieste, Italy*

[g] *Dipartimento di Fisica Generale, Università di Torino, via P. Giuria 1 Torino, Italy, and INFN Sez. di Torino, via P. Giuria 1 Torino, Italy*

[h] *INFN Sez. di Torino, via P. Giuria 1 Torino, Italy*

[i] *ENEA, Frascati, Italy*

[j] *Dip. di Fisica Univ. di Bari, via Amendola 179 Bari, Italy and INFN Sez. di Bari, via Amendola 179 Bari, Italy*

[k] *Dipartimento di Fisica, Università di Bologna, via Irnerio 46, Bologna, Italy and INFN, Sezione di Bologna, via Irnerio 46, Bologna, Italy*

[ℓ] *INFN Sez. di Pavia, via Bassi 6 Pavia, Italy*

[m] *Dep. of Physics Univ. of Tokyo, Bunkyo Tokyo 113-0033, Japan*

[n] *INFN, Sez. di Trieste, via Valerio 2 Trieste, Italy*

[o] *JINR, Dubna, Moscow region, Russia*

[p] *Dep of Physics Shahid Behesty Univ., 19834 Teheran, Iran*

[q] *INAF-IFSI Sez. di Torino, C.so Fiume, Torino, Italy and INFN Sez. di Torino, via P. Giuria 1 Torino, Italy*

[r] *High Energy Accelerator Research Organization (KEK), Tsukuba, Ibaraki 305-0801, Japan*

[s] *TRIUMF, 4004 Wesbrook Mall, Vancouver BC V6T 2A3, Canada*

[t] *RIKEN, Wako, Saitama 351-0198, Japan*

[u] *INFN Sez. di Bari, via Amendola 179 Bari, Italy*

[v] *Dip. di Meccanica, Università di Brescia, via Valotti 9 Brescia, Italy and INFN Sez. di Pavia, via Bassi 6 Pavia, Italy*

**Abstract**

The FINUDA spectrometer has recently been used to perform a wide physics program at DAΦNE, the Frascati Φ-factory. The slow negative Kaons from the $\phi(1020)$ decays were stopped in several nuclear targets and the formation and decay products of strange hadronic systems were detected by FINUDA. Some highlights of the ongoing analysis will be shown regarding the spectroscopy of Λ-hypernulei, the search for Σ-hypernuclei and that of deeply-bound kaonic nuclei.

## 1 Introduction

The FINUDA experiment is a nuclear physics, fixed target experiment which is being carried out at DAΦNE, the Φ-factory in operation at the I.N.F.N. National Laboratories of Frascaty (Italy). DAΦNE is an $e^+e^-$ collider whose beams are tuned at an energy of 510 MeV in order to produce $\phi(1020)$ mesons at rest. FINUDA makes use of the low energy ($\sim$16 MeV) negative kaons from the $\phi \to K^+K^-$ decay channel to perform nuclear physics studies in the strange sector. The advantages of such a novel approach are manyfold, the main ones being the low hadronic backgrounds and the large coverable solid angle. With FINUDA it is possible to simultaneously study the formation and decay of strange hadronic systems with good momentum resolution and on different targets. The FINUDA design, optimized to perform high resolution spectroscopy and studies of the mesonic and non-mesonic decays of

[1] deceased

Λ-hypernuclei, is very well suited for carrying out searches in a variety of strange physics topics, especially where the backgroud rejection and the identification of specific systems rely upon a complete reconstruction of complex events.

## 2 The FINUDA Experiment at DAΦNE

The negative kaons from the $\phi$ decay are a very peculiar type of "beam", presenting several advantages with respect to extracted beams. Since the $\phi(1020)$ is produced at rest, the $\phi \to K^+K^-$ decay is characterized by a back-to-back topology. The $K^-$ can therefore be efficiently tagged by detecting in coincidence the associated, backward emitted $K^+$, thus allowing a very efficient background rejection. The low momentum $K^-$'s can be stopped in very thin targets ($\sim$0.2g/cm$^2$) where they can be absorbed by a nucleus and form e.g. a Λ-hypernucleus via the strangeness exchange reaction

$$K^-_{stop} + {}^{A}Z \to {}^{A}_{\Lambda}Z + \pi^- \qquad (1)$$

where ${}^{A}Z$ indicates a target nucleus and ${}^{A}_{\Lambda}Z$ the produced hypernucleus. The prompt $\pi^-$ is negligibly degraded in its way out of the thin target and can therefore be used to make Λ-hypernuclear spectroscopy with high energy resolution. Moreover, the low energy decay products can exit the target and be detected, thus allowing the study of the weak decay of the formed hypernucleus. More in general it possible to detect the formation and decay products of any strange, nuclear interacting system formed subsequently to the stopping of the negative kaon, as described in the following sections. This can be achieved by exploiting the tracking and momentum resolution capabilities of the FINUDA spectrometer. Fig. 1 shows a global view of the apparatus. The layers of the tracker are contained inside a superconducting solenoid, which provides a highly homogeneous (better than 2% ) magnetic field of 1.0 T over a cylindrical volume of 146 cm radius and 211 cm length. Three main regions can be distinguished inside the FINUDA apparatus.

- *The interaction/target region* is shown schematically in fig. 2. The highly ionizing $(K^+, K^-)$ pairs are detected by a barrel of 12 thin scintillator slabs (TOFINO), surrounding the beam pipe. The high energy, back-to-back response in the TOFINO slabs is used for trigger purposes and time measurements. The kaons are then traced by means of an octagonal array of silicon microstrip detectors (ISIM) before entering the targets, which face the silicon detectors at a distance of a couple of millimeters. The spatial resolution of the ISIM detector is $\sim 30\mu$m and this allows, thanks also to the thinness of the targets, to determine the interaction point of the kaons with a

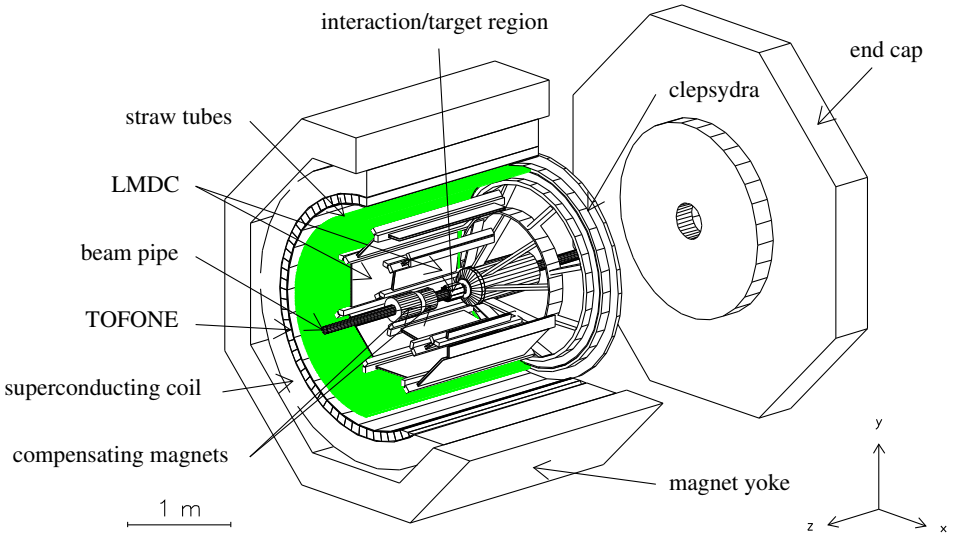


Fig. 1. Global view of the FINUDA detector.

precision of $\sim$ 800 hundred microns. This precision is essentially limited by the range straggling of the kaons in the last part of their path. The silicon microstrip detector is also used for mass discrimination purposes, having an energy resolution of $\sim$ 25% [1] for the kaons from $\phi$ decay.

- *The external tracking device* consists of four layers of position sensitive detectors, arranged with cylindrical symmetry around the beam pipe axis. A He atmosphere is introduced in the tracking volume to reduce the effects of the multiple Coulomb scattering on the charged tracks. The tracking detectors are the following, in increasing radius order: (i) an array of ten double-sided silicon microstrip modules (OSIM) placed close to the targets (see fig. 2) and used also for mass discrimination purposes; (ii) two arrays of eight planar low-mass drift chambers (LMDC) filled with a (70%He-30%$C_4H_{10}$) mixture, featuring a spatial resolution of $\sigma_{\rho\phi} \sim 150$ $\mu$m and $\sigma_z \sim 1.0$ cm [2]; (iii) a straw tube detector placed at a radius of $\sim$ 1.1m and composed by six layers of longitudinal and stereo tubes, which provides a spatial resolution of $\sigma_{\rho\phi} \sim 150$ $\mu$m and $\sigma_z \sim 500$ $\mu$m [3].
- *The external time of flight barrel* (TOFONE) is composed of 72 scintillator slabs, 10 cm thick and 255 cm long, and provides signals for the first level trigger and for the measurement of the time-of-flight of the charged particles. Moreover, it is used for the detection of neutrons with an efficiency of $\sim$10%, an angular acceptance of 70% and an energy resolution of 8 MeV FWHM for neutrons of 80 MeV [4].

The above mentioned performances together with its large acceptance allow FINUDA to simultaneously study the formation and decay of strange hadronic systems via a full and exclusive event recontruction, which makes of FINUDA a rather unique apparatus in the field of hypernuclear physics. Further details concerning the design and performances of the FINUDA apparatus can be found in [5–7].

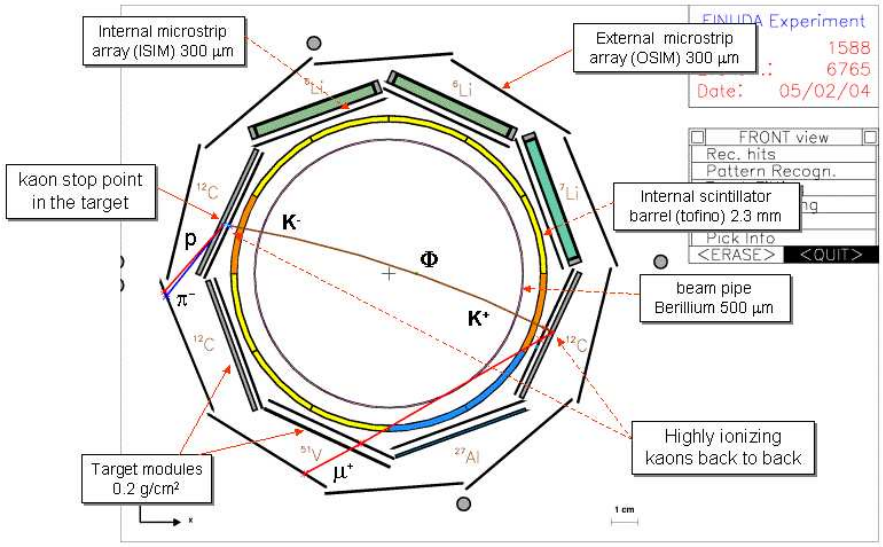


Fig. 2. Schematic view of the interaction/target region

FINUDA can host eight different targets (see fig. 2) with the possibility of obtaining data on different hypernuclei at the same time. A set of light targets was chosen for the first data taking period, since there the rich K-nucleus dynamics is cleaner and easier to study. in particular they are an ideal ground where to perform weak decay studies of Λ-hypernuclei and also the best candidates where to search for Σ-hypernuclei or for the formation of deeply bound kaonic states. Some heavier targets were also used to allow the study of A-dependencies and to test the pheasibility of future studies on heavy nuclei. The following targets were selected: two $^{6}$Li (isotopically enriched to 90%), one $^{7}$Li (natural isotopic abundance), three $^{12}$C, one $^{27}$Al and one $^{51}$V. The carbon targets were also used for calibration purposes since they are the most studied ones.

## 3 Data taking and detector performances

After the commissioning of the spectrometer a period of data taking started in december 2003 and ended in March 2004. The trigger used to select hypernuclear events required two back-to-back TOFINO slabs to provide a signal above the kaon threshold and a fast coincidence with the TOFONE barrel. This allowed to select highly ionizing $K^+K^-$ pairs in coincidence with a fast outgoing particle against backgrounds coming from the other $\phi$ decays or generated by the accelerator electromagnetic background. The procedure to reconstruct procedure of the $\phi$ formation point and of the kaon directions and momenta uses the kaons interaction points in the ISIM modules, identified

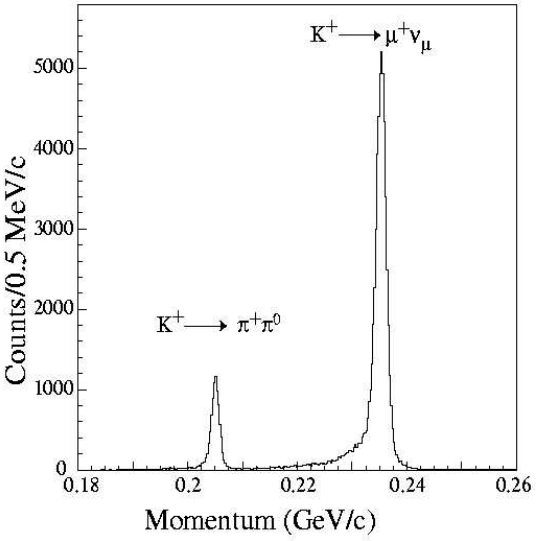


Fig. 3. Momentum distribution of the positive tracks originated in the stopped $K^+$ vertex. The peak at 236 MeV/c corresponds to the two body decay $K^+ \to \mu^+\nu_\mu$, the peak at 205 MeV/c corresponds to the two body decay $K^+ \to \pi^+\pi^0$.

through their high stopping power. Hypernuclear events are selected by the simultaneous detection of a $K^+$ and a $K^-$. The presence of a $K^+$, besides allowing the $K^-$ tagging, offers the possibility to perform an accurate and continuous in-beam calibration of FINUDA. The positive kaons, stopping in the target array, decay at rest with a mean life of 12.4 ns. The two main two-body decays $K^+ \to \mu^+\nu_\mu$ (63.51%) and $K^+ \to \pi^+\pi^0$ (21.16%) are a source of monochromatic particles crossing the spectrometer with momenta of 235.5 MeV/c for the $\mu^+$ and of 205.1 MeV/c for the $\pi^+$, respectively. The absolute scale of the momenta was determined with a precision better than 200 keV/$c$, which can be assumed as the systematic error on the measurement of the particles momenta in the range between 200 and 300 MeV/$c$.
Fig. 3 shows the momentum distribution of the positive tracks originated in the stopped $K^+$ vertex. The two peaks at 236 MeV/c and 205 MeV/c correspond to the previously mentioned decays. From the width of the $\mu^+$ peak the present momentum resolution of the apparatus can be estimated to be $\Delta p/p$=0.6% FWHM. The momentum resolution of the spectrometer is expected to improve to the design value of 0.4% FWHM after the final detector calibration and alignment will be performed.

## 4 Results on $^{12}_{\Lambda}$C spectroscopy.

In order to evaluate the capabilities of FINUDA to yield relevant spectroscopic parameters, the analysis started on $^{12}$C targets. Due to some residual systematic problems on one carbon target the current analysis is based on a partial set of data. An excitation spectrum with a 1.45 FWHM resolution

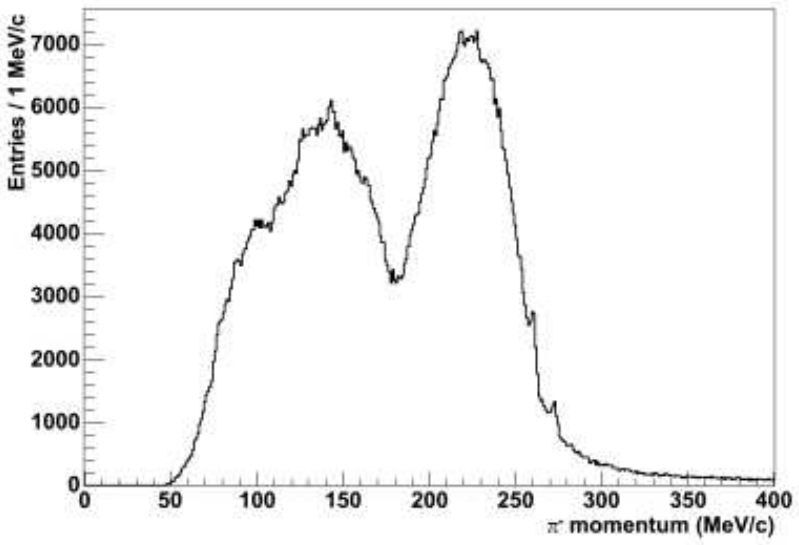


Fig. 4. Momentum spectrum of the $\pi^-$ emitted after the interaction of a $K^-$ with a $^{12}$C target.

was recently obtained at KEK for $^{12}_{\Lambda}$C using the ($\pi^+$, $K^+$) reaction at 1.05 GeV/$c$ by the E369 Collaboration [9]. The raw momentum spectrum of the $\pi^-$ coming from the analysed $^{12}$C targets is shown in Fig. 4. The main processes that produce $\pi^-$ after $K^-$ absorption [11] are:

a) quasi-free $\Sigma^+$, $\Sigma^0$ and $\Lambda$ production: $K^-p \rightarrow \Sigma^+\pi^-$, $K^-n \rightarrow \Sigma^0\pi^-$, $K^-n \rightarrow \Lambda\pi^-$;
b) quasi-free $\Lambda$ decay: $\Lambda \rightarrow p\pi^-$;
c) quasi-free $\Sigma^-$ production: $K^-p \rightarrow \Sigma^-\pi^+$, followed by $\Sigma^- \rightarrow n\pi^-$;
d) two nucleon $K^-$ absorption: $K^-(NN) \rightarrow \Sigma^- N$, followed by $\Sigma^- \rightarrow n\pi^-$.

All the mentioned reactions were simulated in the FINUDA Monte Carlo program and the $\pi^-$ momentum distribution at production of the full simulation can be seen in fig. 5. The simulated events were later filtered by the reconstruction program with the same selection criteria as for the real events, in order to take into account the acceptance and the reconstruction efficiency of the apparatus. In the momentum region where the bound states of $^{12}$C are expected to appear (beyond $\sim$ 260 MeV/$c$), only process d) is contributing. In order to obtain the $\Lambda$ binding energy distribution the d) process is subtracted from the $\pi^-$ momentum distribution, and the momenta are converted into binding energies ($-B_\Lambda$). These results show that the method of producing hypernuclei by stopping the low energy $K^-$ from $\phi$ decay in thin nuclear targets proved to work, and may be used to perform accurate measurements on many hypernuclear observables, which is going to be made on the whole set of nuclear targets used.

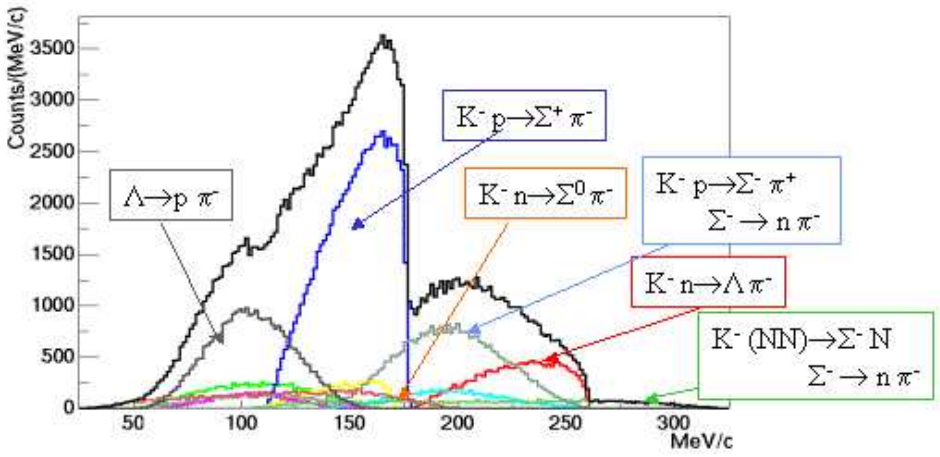


Fig. 5. Simulated inclusive momentum spectrum of the $\pi^-$ emitted after the interaction of a $K^-$ with a $^{12}$C target. The contributions from the different quasi-free reactions are indicated in the figure

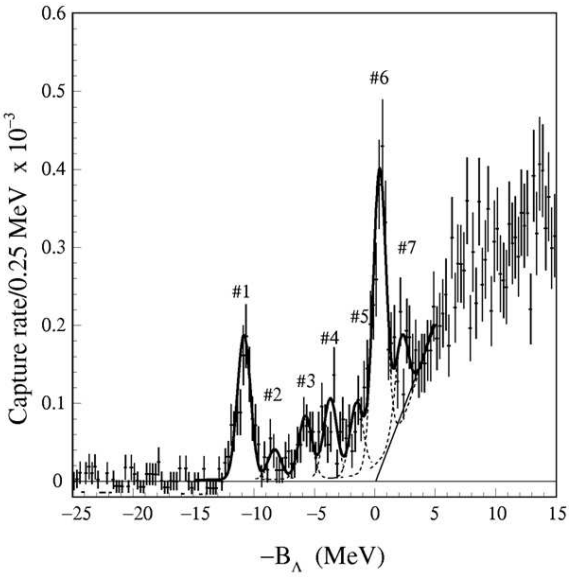


Fig. 6. $\Lambda$ binding energy spectrum of $^{12}_{\Lambda}C$ measured by the FINUDA experiment. The solid line represents the result of a fit with 7 gaussian functions as explained in the text. The solid line starting at $B_\Lambda = 0$ MeV represents the contribution from the quasi-free $\Lambda$ production.

The two prominent peaks in fig. 6 at $B_\Lambda$ around 11 MeV (ground state) and 0 MeV, have already been observed in previous experiments [12,13] and inter-

| Peak number | $-B_\Lambda$ (MeV) | Capture rate/(stopped $K^-$)[$\times 10^{-3}$] |
|---|---|---|
| 1 | $-10.94 \pm 0.06$ | $1.01 \pm 0.11_{stat} \pm 0.10_{syst}$ |
| 2 | $-8.4 \pm 0.2$ | $0.21 \pm 0.05$ |
| 3 | $-5.9 \pm 0.1$ | $0.44 \pm 0.07$ |
| 4 | $-3.8 \pm 0.1$ | $0.56 \pm 0.08$ |
| 5 | $-1.6 \pm 0.2$ | $0.51 \pm 0.08$ |
| 6 | $0.27 \pm 0.06$ | $2.04 \pm 0.15$ |
| 7 | $2.1 \pm 0.2$ | $0.59 \pm 0.11$ |

Table 1
Results from $-B_\Lambda$ spectrum fits with 7 hypernuclear levels. The last column reports the capture rates corresponding to each peak. The errors reported for peak (#2÷#7) do not include the error on the ${}^{12}_{\Lambda}$C ground state capture rate.

preted as $(\nu p^{-1}_{\frac{1}{2}}, \Lambda s)$ and $(\nu p^{-1}_{\frac{3}{2}}, \Lambda p)$ ($\nu$= nucleon). The experimental energy resolution was determined by fitting the $B_\Lambda \simeq 11$ MeV peak with a gaussian curve, and amounts to 1.29 MeV FWHM. The experimental spectrum closely resembles the one from E369 experiment [9]. In between the two main peaks, there are also indications of other states produced with weaker strength. In order to reproduce this spectrum seven gaussian functions were used; the widths were fixed, for all of them, to $\sigma = 0.5$ MeV, corresponding to the present experimental resolution and leaving the positions of the seven levels free. The result of this fit is shown in Fig. 6 and their values are reported in Tab.1 together with the calculated relative capture rate. A contribution from the quasi-free $\Lambda$-production, starting from $B_\Lambda = 0$, was included in both fits. These results show that the method of producing hypernuclei by stopping the low energy $K^-$ from $\phi$ decay in thin nuclear targets proved to work, and may be used to perform accurate measurements on many hypernuclear observables, which is going to be made on the whole set of nuclear targets used.

## 5 The search for $\Sigma$-bound states

A $K^-$ impinging upon a nucleus can transform one of its nucleons into a hyperon; unlike the $\Lambda$ case, if the hyperon is a $\Sigma$ it can decay via strong interaction through the $\Sigma N \to \Lambda N$ conversion reaction. Since the width associated to this mechanism was originally expected to be about 25 MeV [15], $\Sigma$-bound states were not expected to exist. Nevertheless at least one $\Sigma$ hypernucleus, ${}^{4}_{\Sigma}He(\Sigma \equiv \Sigma^{0,+})$ has been definitely identified [16] with a width $\Gamma \sim 6MeV$. This unexpected finding has been explained [17] as related to the interplay between a strong isospin dependent Lane term of the $\Sigma$-nucleus potential and the presence of a central repulsion which keeps the $\Sigma$ out of the nucleus

enough for the conversion reaction to be suppressed. Whether $\Sigma$-bound states exist on heavier nuclei is still controversial, depending on the poorly known $\Sigma$-nucleus potential, which is considered to be attractive by some authors [18] and repulsive by others [19]. Moreover, in order for the $\Sigma$-bound states to be experimentally detectable, there should exist mechanisms suppressing the strong $\Sigma$ absorption inside nuclear matter in order for their width to be smaller than the energy separation between levels. According to the model predictions of [18] the proper accounting of the spin-isospin polarization of the nuclear medium related to the $\Sigma N \rightarrow \Lambda N$ transition and of other mechanisms such as Pauli blocking, narrow down the width enough ($\sim$7MeV) to make the $\Sigma$-bound states detectable.
Several experimental efforts were devoted to the search of $\Sigma$-hypernuclei via $(\pi, K)$ and $(K, \pi)$ reaction studies [20] but no clear and unquestionable evidence has been found up to now on nuclei other than $^4He$. The detection of $\Sigma$ hypernuclear states by means of inclusive measurements is not a trivial task; such an approach may infact not result suitable for separating several MeV broad structures from rather complex and overwhelming quasi-free backgrounds (see e.g. in fig. 5 the $\pi^-$ momentum region around 170 MeV/c where these states are expected to appear). FINUDA can reconstruct the whole hypernuclear event since it can simultaneously detect the formation and decay of $\Sigma$-hypernuclei via $(K^-_{stop}, \Lambda\pi)$ reaction. In FINUDA a $\Sigma$-hypernucleus should be detected after formation via the production reaction

$$K^-_{stop} + ^A Z \rightarrow ^A_{\Sigma^{\pm},0} Z' + \pi^{\mp} \tag{2}$$

The $\Sigma$ hyperon subsequently converts into a $\Lambda$ via the $\Sigma N \rightarrow \Lambda N$ reaction generally giving the $\Lambda$ enough energy to escape the nucleus and decay in the free space. A simulation of a $\Sigma^-$ production event on $^{12}C$ in FINUDA can be seen in fig. 7. Two vertices can be distinguished: the first one is characterized by the topology of the $^{12}_{\Sigma^-}Be$ production, while the second shows the $\Lambda \rightarrow \pi^- p$ decay following the conversion reaction. The strategy to identify such events is based on the following procedure: i) detection of a prompt pion signalling the formation of the hypernucleus; ii) further selection of events in coincidence with a $(\pi^- p)$ couple exitting from a secondary vertex and matching the invariant mass of a $\Lambda$; iii) the secondary vertex is required to be physically distinct from the primary one. The present analysis will focus on the search for the reaction

$$K^-_{stop} + ^{12} C \rightarrow ^{12}_{\Sigma^+} C + \pi^- \tag{3}$$

followed by the conversion reaction and the subsequent $\Lambda$ decay:

$$^{12}_{\Sigma^+}C \rightarrow ^{10} B + \Lambda + p, \qquad \Lambda \rightarrow \pi^- + p. \tag{4}$$

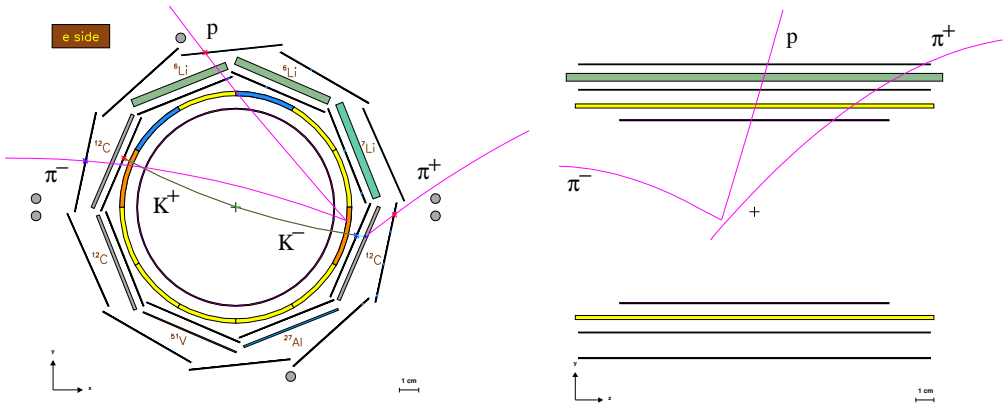


Fig. 7. Front view of the FINUDA detector vertex region with a reconstructed $\Sigma^-$ hypernuclear event: $K^-_{stop} + ^{12}C \rightarrow ^{12}_{\Sigma^-}Be + \pi^+$ followed by $^{12}_{\Sigma^-}Be \rightarrow ^{10}Be + \Lambda + n$ and finally by $\Lambda \rightarrow \pi^- + p$ .

The $\Sigma$-hypernuclei spectroscopy is based on the analysis of the $\pi^-$ momentum distribution; in figure 4 the inclusive $\pi^-$ spectrum from the $K^-_{stop} + ^{12}C \rightarrow \pi^- X$ reaction is shown. No evidence of bound states can be extracted from the quasi-free background in the region of ∼150-200 MeV/c, where they are expected to appear. In fig. 8(empty histogram) the $\pi^-$ momentum spectrum is shown after requesting a coincidence with a ($\pi^-$ p) couple whose invariant mass matches that of a $\Lambda$. The resulting yield of the quasi-free background is reduced by almost three orders of magnitude (compare to fig. 4) by applying such conditions and two peaks appear in the 150-200 MeV/c region. In order to subtract the background, the quasi-free simulated background described in the previous section and integrated with $\Sigma$ conversion reactions and pion rescattering, was filtered through the FINUDA reconstruction program and the resulting momentum spectrum was normalized to the experimental one. This can be seen in fig. 8 (shadowed histogram) where the main $\Sigma$ and $\Lambda$ quasi-free production contributions are visible as two wide bumps at low and high $\pi^-$ momentum respectively.
The resulting, background subtracted spectrum is shown in figure 9. Two adjacent peaks appear in the spectrum, which are the candidate $\Sigma$ bound states. If interpreted as a signature of $^{12}_{\Sigma^+}$C, they would correspond to $\Sigma^+$ binding energies (widths) of 13 MeV (7MeV) for the higher and 2MeV (7MeV) for the lower momentum bump. The $\Sigma^0$ is not taken into account here since it is known to have a formation probability which is only $\sim$ 10% of that of the $\Sigma^+$. The existence of a $\Sigma^+$ bound state was earlier predicted by [18], yielding a binding energy and width of 7.5 MeV and 6.7 MeV respectively for the 1s orbital. A similar analysis is in progress also on other charge channels and targets, and it appears to give similar results.

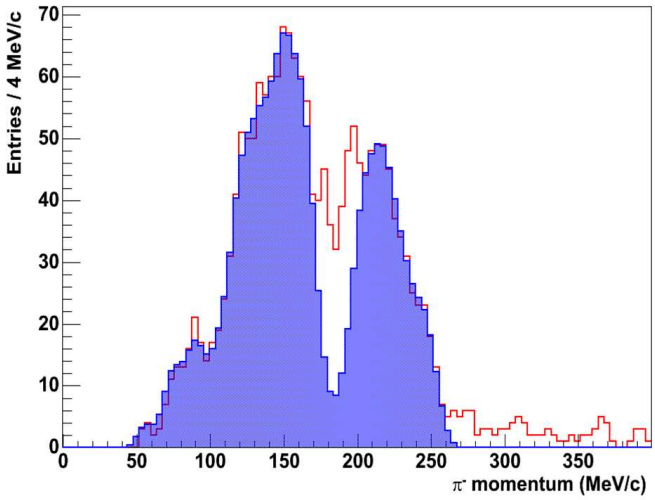


Fig. 8. Continuous histogram: momentum distribution of $\pi^-$'s when in coincidence with ($\pi^-$p) pairs with invariant mass matching the $\Lambda$ mass. Shaded histogram: simulated quasi-free background.

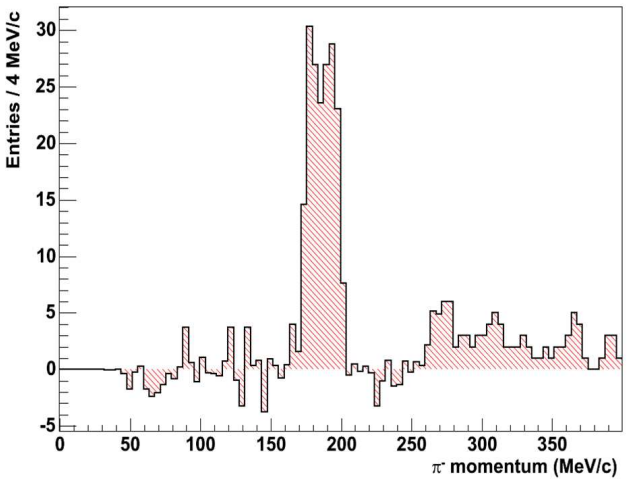


Fig. 9. backgroung subtracted momentum distribution of $\pi^-$'s when in coincidence with ($\pi^-$p) pairs with invariant mass matching the $\Lambda$ mass.

## 6 Study of kaon-bound $K^-pp$ states

Whether $\overline{K}$-nucleus bound states exist or not crucially depends on the shape of the $\overline{K}$-nucleus optical potential. There is no common understanding about its value, and while some authors deduce a shallow potential [21] from the experimental data others [22,23] claim it is very deep. If the $K^-$-nucleus potential is as deep as 200MeV $\overline{K}$-nucleus bound states could be experimentally visible. In a recent work [22] Akaishi and Yamazaki discussed the possibility of formation of discrete nuclear $\overline{K}$ bound states in few body systems. By taking into account $\overline{K}$N scattering lengths and the kaonic hydrogen data and considering the $\Lambda(1405)$ as a $\overline{K}$N bound system, they derived a very deep $\overline{K}$ nucleus

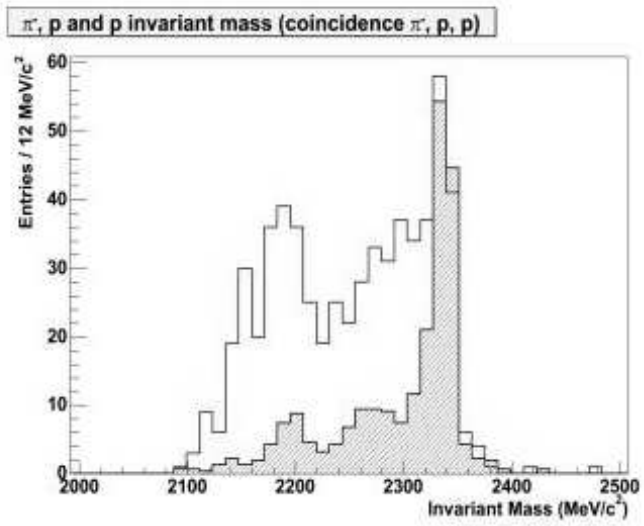


Fig. 10. Experimental (open histogram) and simulated (shadowed histogram) $\Lambda p(\pi^- pp)$ invariant mass distribution for $\Lambda p$ back-to-back events. The two histograms have been normalized at $\sim$ 2.34 GeV (see text for further details).

interaction. The resulting binding energies for these light systems are so large ($\geq$ 80MeV) that the main decay channel of the I=0 $\overline{K}$N pair to $\Sigma\pi$ is forbidden; as a consequence the deeply bound state becomes narrow enough ($\sim$ 20 MeV for the $^{3}_{K}H$ state) to be experimentally visible. Recently two experimental groups reported [24] possible signatures of deeply bound kaonic states, namely of $^{15}_{K^-}O$ and of $(K^- ppn)$ and $(K^- pnn)$bound states. These experiments are missing-mass experiments of the type A(K$^-$,N)X and some ambiguities remain whether the K$^-$ was really bound or not. With FINUDA the invariant mass of the bound system can be directly measured by detecting its decay products. Our initial study is focussed on the search for a deeply-bound $K^- pp$ system. When a K$^-$ interacts with two protons, one expects a hyperon-nucleon pair ($\Lambda$+p, $\Sigma$+N) to be emitted with a back-to-back angular correlation, ignoring final state interactions. Our analysis is foccused on the search of $\Lambda$p, back-to-back events and is based on the following steps: i) selection of $pp\pi^-$ events; ii) selection of $(p\pi^-)$ pairs with invariant mass corresponding to the $\Lambda$ mass; iii) selection of $\Lambda - p$ pairs emitted with back-to-back opening angle ($\cos\theta_{open} \leq$0.8). The $\theta_{open}$ opening angle distribution between a $\Lambda$ and a proton (not shown) is strongly peaked around $\cos(\theta_{open})$=1, which clearly indicates that most of the $\Lambda p$ events are coming from an intermediate "$K^- pp$"system almost at rest. If the reaction process were simply a two-nucleon absorption process, the mass of the system should be close to the sum of a kaon and two proton masses, namely 2.37 GeV/c$^2$, minus the separation energy of the two protons, which amounts to approximately 30 MeV. A significant mass decrease

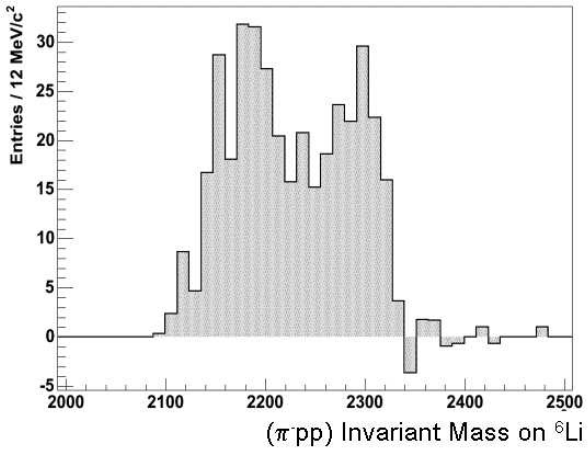


Fig. 11. $\Lambda p(\pi^- pp)$ invariant mass distribution for $\Lambda p$ back-to-back events after subtraction of simulated background

of the $K^- pp$ system is observed instead (see fig. 10), with a lot of strength accumulated below the $K^- pp$ absorption peak. The shadowed histogram is the result of the background simulation filtered with the same reconstruction cuts as the experimental data. The main contribution to the background comes from the $K^- pp \to \Lambda + p$ two nucleon absorption which shows up as a peak at about 2.34 GeV. The background was subtracted after normalizing it to the experimental data at the $K^- pp \to \Lambda + p$ absorption peak. The result is shown in fig. 11: the $\Lambda - p$ invariant mass distribution is sensibly shifted toward lower values with respect to the absorption peak with two wide structures peaked at about 2.290 GeV and 2.190 GeV, 50 MeV and 75 MeV wide respectively (Lorentzian fit). The higher peak can be interpreted as a $K^- pp$ bound state, with a binding energy of approximately 90 MeV (value obtained without applying any acceptance correction). Events from $K^- pp \to \Sigma^0 + p$ can contribute to the $\Lambda p$ invariant mass via the $\Sigma^0 \to \Lambda\gamma$ decay: they should still present a $\Lambda$p back-to-back correlation and the distribution should be shifted by $\sim$74 MeV and broadened because of the missing $\gamma$. Although the observed separation between the two experimental bumps is greater than 74 MeV, the lower bump could be attributed to such decay. It should be noted infact that no acceptance correction has been applied yet, which will possibly affect both the shape and position of both bumps. These corrections are presently under way as well as a further refinement of the analysis.

## 7 Summary

We have presented some results from the analysis presently being performed on data collected at the DA$\Phi$NE $\phi$-factory with the FINUDA spectrometer. FINUDA makes use of the low energy, monocromatic $K^-$ produced by the $\phi$ decay into $K^+K^-$ pairs to perform a wide program of studies in the strange sector by stopping the kaons in different nuclear targets arranged around the beam pipe. Notable is the capability of FINUDA to fully reconstruct multi-track events with high momentum resolution, which allows to dramatically reduce backgrounds and make exclusive measurements. The first effort was put in the analysis of the $\Lambda$ hypernuclei formation on $^{12}$C. The analysis results compare well with the best existing literature data, which allowed us to prove FINUDA's ability to perform high resolution hypernuclear spectroscopy. Data analysis on several different nuclear targets is under way.

Another topic which was presented is the search for $\Sigma$ hypernuclei. Unlike existing inclusive literature data, FINUDA is able to perform exclusive measurements by fully reconstructing the $\Sigma$-hypernuclei formation and decay. In particular, FINUDA can detect the pion from the $\Sigma$-hypernucleus production $K^-_{stop} + {}^A Z \rightarrow {}^A_{\Sigma^{\pm},0} Z + \pi^{\mp}$ and use it for spectroscopy measurements. It can also simultaneously detect the $\Lambda$ emitted by the subsequent $\Sigma N \rightarrow \Lambda N$ conversion reaction by identifying its decay products $(\pi^- p)$ as coming from a secondary vertex. The use of these very selective conditions allowed us to dramatically reduce the inclusive background and to evidenciate two possible candidate ${}^{12}_{\Sigma^+}$C bound states, corresponding to $\Sigma^+$ binding energies of 13 MeV and 2 MeV and widths of $\sim$7 MeV. The analysis is still in progress, but similar evidences are being found in other charge channels too.

The last topic presented regards the search for deeply bound kaonic nuclei. Recent experiments [24] found, via missing mass A(K$^-$,N)X measurements, possible signatures of such states, which have been predicted to be bound by as much as $\sim$100 MeV in the case of light nuclei. We have searched for kaon-bound $(K^- pp)$ states by studying the invariant mass of a possible decay channel, namely $\Lambda - p$ events emitted back-to-back. Although the analysis is not final, and in particular no acceptance corrections have been made yet, it can be stated that the $\Lambda - p$ invariant mass distribution presents a strong accumulation of strength below the $(K^- pp)$ total free mass. A rather wide structure peaked at about 2290 MeV can be interpreted as the evidence of a $(K^- pp)$ state bound by as much as $\sim$90 MeV. If confirmed by further analysis this would be the first time a similar object is directly seen.

## References


[1] Bottan P. *et al.*, *Nucl. Instr. Methods* **A427** (1999?, 423

[2] Agnello M. *et al.*, *Nucl. Instr. Methods* **A385** (1997), 58

[3] Benussi L. *et al.*, *Nucl. Instr. Methods* **A361** (1995), 180; Benussi L. *et al.*, *Nucl. Instr. Methods* **A419** (1998), 648

[4] Pantaleo A. *et al.*, *Nucl. Instr. Methods* **A**, accepted for publication

[5] Zenoni A., in *Physics and Detectors at DA$\Phi$NE*, Frascati Physics Series Vol. XVI (1999), edited by Bianco S. et al., p. 739

[6] Gianotti P., *Nucl. Phys.* **A691** (2001), 483c

[7] Zenoni A. and Gianotti P., *Europhysics News* **33/5** (2002), 157

[8] Innocente V. et al., *GEANE: Average Tracking and Error Propagation Package*, CERN Program Library, W5013-E (1991)

[9] Hotchi H. *et al.*, *Phys. Rev.* **C64** (2001), 044302

[10] Schaffner-Bielich *et al.*, Nucl.Phys. **A669** (2000); Ramos *et al.*, Nucl. Phys. **A671** (2000) 481, Cieply *et al.*, Nucl.Phys. **A696** (2001), 173

[11] Tamura H. *et al.*, *Prog. Th. Phys. Suppl.* **117** (1994), 1

[12] Faessler A.M. *et al.*, *Phys. Lett.* **46B** (1973), 468

[13] Sakaguchi A. *et al.*, *Phys. Rev.* **C34** (1991), 73; Tamura H. *et al.*, *Nuovo Cim.* **A102** (1989), 575

[14] Itonaga K. *et al.*, *Prog. Theor. Phys.* **84** (1990), 291

[15] Batty C.J.*et al.*, Phys. Lett. **B74** (1978) 27.

[16] Bertini R.*et al.*, Phys.Lett **B90**(1980)375; Hayano R.S. *et al.*, Phys. Lett. **B231** (1989), 355; Nagae T, *et al.*, Phys.Rev Lett. **80** (1998), 1605

[17] Harada T.*et al.* Nucl. Phys. **A507** (1990), 715

[18] Oset E. *et al.*, Phys.Rep. 188,2 (1990), 79

[19] Mares J. *et al.* Nucl. Phys. **A594** (1995), 311

[20] Yamazaki T. *et al.*, Phys. Rev. Lett. **54** (1985) 102; Yamazaki T. *et al.*, Nucl. Phys. **A450** (1986) 1c; Hayano R.S. *et al.* Nucl. Phys. **A478** (1988) 113c.

[21] Schaffner-Bielich *et al.*, Nucl.Phys. **A669** (2000); Ramos *et al.*, Nucl. Phys. **A671** (2000) 481, Cieply *et al.*, Nucl.Phys. **A696** (2001), 173

[22] Akaishi *et al.* Phys. Rev. **C65** (2002), 044005

[23] Kaiser *et al.*, Nucl. Phys. **A594** (1995), 325

[24] Iwasaki M. *et al.*, nucl-ex/0310018, Suzuki T. *et al.*, Phys.Lett. **B 597**(2004), 263